Polycomb and Hox Genes Control JNK-Induced Remodeling of the Segment Boundary during Drosophila Morphogenesis

Solange Roumengous, Raphaël Rousset, S. Noselli

Article

Cell Reports

Polycomb and Hox Genes Control JNK-Induced Remodeling of the Segment Boundary during *Drosophila* Morphogenesis

Graphical Abstract

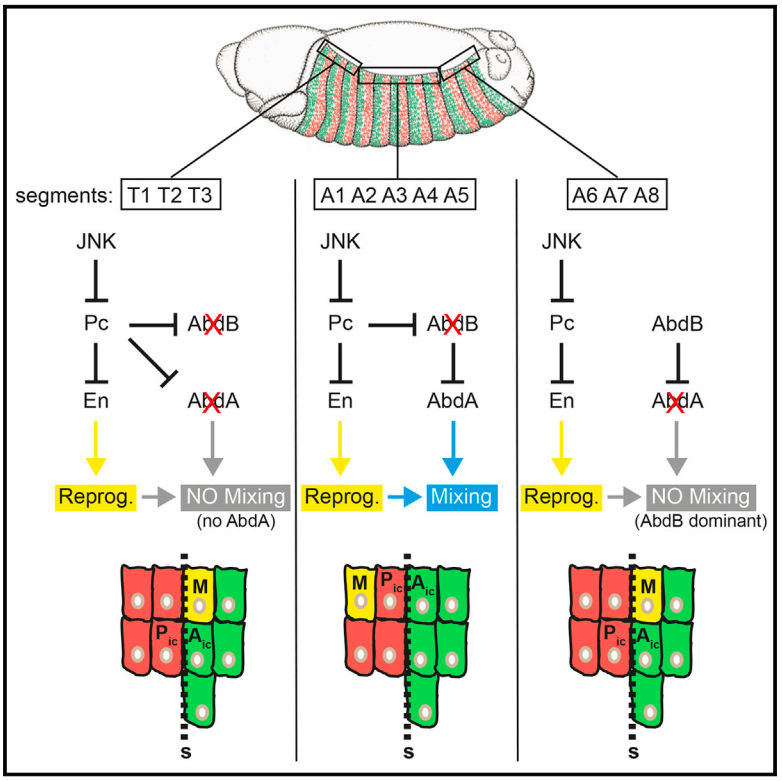

Highlights

- JNK controls Mixer cell reprogramming through *Polycomb* downregulation
- HOX genes spatially regulate cell mixing at segment boundaries
- *Abdominal-A* acts as a pro-mixing factor
- *Abdominal-B* is a prevalent, negative regulator of cell mixing

Authors

Solange Roumengous, Raphaël Rousset, Stéphane Noselli

Correspondence

rousset@unice.fr (R.R.), noselli@unice.fr (S.N.)

In Brief

Roumengous et al. identify a gene regulatory network involving JNK, *Polycomb*, *engrailed*, and Hox genes that is important for developmental reprogramming and cell remodeling during tissue morphogenesis.

Roumengous et al., 2017, Cell Reports *19*, 60–71
April 4, 2017
http://dx.doi.org/10.1016/j.celrep.2017.03.033

CellPress

OPEN ACCESS
CellPress

Cell Reports
Article

Polycomb and Hox Genes Control JNK-Induced Remodeling of the Segment Boundary during *Drosophila* Morphogenesis

Solange Roumengous,[1] Raphaël Rousset,[1,*] and Stéphane Noselli[1,2,*]
[1]Université Côte d'Azur, CNRS, INSERM, iBV, 06108 Nice, France
[2]Lead Contact
*Correspondence: rousset@unice.fr (R.R.), noselli@unice.fr (S.N.)
http://dx.doi.org/10.1016/j.celrep.2017.03.033

SUMMARY

In segmented tissues, anterior and posterior compartments represent independent morphogenetic domains, which are made of distinct lineages separated by boundaries. During dorsal closure of the *Drosophila* embryo, specific "mixer cells" (MCs) are reprogrammed in a JNK-dependent manner to express the posterior determinant *engrailed* (*en*) and cross the segment boundary. Here, we show that JNK signaling induces de novo expression of *en* in the MCs through repression of *Polycomb* (*Pc*) and release of the *en* locus from the silencing PcG bodies. Whereas reprogramming occurs in MCs from all thoracic and abdominal segments, cell mixing is restricted to the central abdominal region. We demonstrate that this spatial control of MC remodeling depends on the antagonist activity of the Hox genes *abdominal-A* and *Abdominal-B*. Together, these results reveal an essential JNK/*en*/*Pc*/Hox gene regulatory network important in controlling both the plasticity of segment boundaries and developmental reprogramming.

INTRODUCTION

During normal development, progenitor cells differentiate into specific cell types through a robust and essentially irreversible process. Nevertheless, some cells can retain plasticity, and, in some rare situations, they can change their identity and become reprogrammed into a different cell type. Fate switching can occur through an intermediate progenitor or pluripotent stage. In contrast, during transdifferentiation, cells are reprogrammed to acquire a new cell fate without reversion to a pluripotent state (Graf and Enver, 2009). Transdifferentiation is mostly induced upon in vitro manipulations and during regeneration (Graf, 2011, for a historical review); however, more recent studies indicate that transdifferentiation can also occur in normal development (Gettings and Noselli, 2011; Gettings et al., 2010; Jarriault et al., 2008; Jung et al., 1999; Red-Horse et al., 2010; Shen et al., 2000; Sprecher and Desplan, 2008; Tursun, 2012), raising the question of its function in non-pathological conditions. We have recently shown that in vivo transdifferentiation occurs during dorsal closure in *Drosophila* embryos (Gettings et al., 2010). Dorsal closure is characterized by the dorsal migration of the two lateral ectodermal sheets and their fusion at the midline in order to seal the embryo (Agnès and Noselli, 1999; Noselli, 1998; Young et al., 1993). The JNK signaling pathway is activated in the most dorsal row of ectodermal cells, called the "leading edge" (LE), and is essential for the process (Glise et al., 1995). Our recent work showed that some specific cells of the central abdominal region of the LE, named "mixer cells" (MCs), can cross the segment boundary by moving from the anterior to the adjacent, posterior compartment. This surprising mixing behavior goes against the compartmental boundary rule restricting cell exchanges from compartments made of separate lineages (DiNardo et al., 1988; Larsen et al., 2003). The way MCs break the rule is by de novo expression of the posterior determinant *engrailed* (*en*), thus allowing them to switch their identity from anterior cells to posterior cells. We have shown that this reprogramming event depends on JNK signaling as loss of JNK activity blocks *en* expression and mixing altogether (Gettings et al., 2010). Cell mixing, therefore, represents an interesting model to analyze cell compartmentalization and cell reprogramming/plasticity in vivo. However, how JNK regulates *en* de novo expression and why cell mixing is restricted to the central part of the embryo remain open questions.

The Trithorax-group (trxG) and Polycomb-group (PcG) proteins form complexes with transcription factors to regulate the chromatin state and transcription (Geisler and Paro, 2015; Schuettengruber et al., 2007). PcG proteins form two multimeric complexes (PRC1 and PRC2) that act on chromatin compaction and methylation (Bantignies and Cavalli, 2011). They bind to specific DNA sequences called PREs (PcG-responsive elements), forming nuclear aggregates named "PcG bodies," in which target genes are silenced (Saurin et al., 1998). Classical PcG target genes are the Homeotic (Hox) genes, known to specify the segment identity along the anterior-posterior (A-P) axis (Bantignies and Cavalli, 2006). Several studies showed that PcG proteins maintain the repressed state of Hox genes outside their domain of expression, allowing a precise pattern of expression along the A-P axis (Lewis, 1978; Soshnikova and Duboule, 2009). Interestingly, the *en* locus contains PREs that are bound by PcG to repress its expression (DeVido et al., 2008; Schuettengruber et al., 2009), thus raising

the possibility that PcG could control *en* in the context of cell mixing during dorsal closure.

In this work, we decipher the genetic program leading to MC transdifferentiation and their pattern of mixing along the A-P axis. We show that JNK signaling represses *en* association to PcG bodies in the nucleus of MCs, thus controlling their transdifferentiation. We further analyzed the contribution of the *Polycomb* (*Pc*) gene in MC formation by looking at the role of its target genes *abdominal-A* (*abdA*) and *Abdominal-B* (*AbdB*). We show that *abdA* is a pro-mixing factor essential for mixing in abdominal segments A1–A5 and that *AbdB* behaves as a strong repressor posteriorly, thus identifying the Hox genes *abdA* and *AbdB* as essential factors in MC patterning along the A-P axis. Our results identify a gene regulatory network involving JNK, *Pc*, *en*, and Hox genes that is important for developmental reprogramming and cell remodeling during tissue morphogenesis.

RESULTS

Two Types of MCs Participate in Dorsal Closure

MCs are integral components of the LE. They are anterior cells with groove-cell identity that are located at the segment boundary (Gettings et al., 2010) (Figure 1A). By using the *odd-skipped* (*odd*) *Gal4* driver (Mulinari and Häcker, 2009), which is specific to groove cells, we could clearly identify the MCs as GFP-positive cells invading the adjacent, GFP-negative, posterior compartment at the end of dorsal closure (Figures 1B and 1C). As previously shown (Gettings et al., 2010), mixing only takes place in the central segments from A1 to A5 (Figure 1C), with MCs expressing *en* de novo (Figures 1D and 1E). We further analyzed the extent of reprogramming by looking at *en* expression in all potential MCs (i.e., all groove cells of the LE from T1 to A8). We observed that, in addition to regular MCs (A1–A5), *en* is also expressed in all other potential MCs from thoracic T1–T3 and abdominal A6–A7 segments (Figure 1F). These observations thus identify two populations of MCs: while both express *en* de novo, some undergo mixing (in segments A1–A5), while others do not (T1–T3; A6–A7). These results further indicate that MC reprogramming, although necessary as previously shown (Gettings et al., 2010), is not sufficient to induce subsequent mixing.

The activity of the JNK pathway in the whole anterior compartment is essential for MC reprogramming and mixing (Gettings et al., 2010). However, it remains unclear whether JNK activity is required and sufficient in the MC itself. To address this question, we used the *oddGal4-GFP* line to manipulate JNK activity specifically in MCs. Inactivating JNK signaling leads to a complete absence of reprogramming and mixing. Indeed, no mixing was observed when blocking JNK activity through overexpression either of *puckered* (*puc*), a negative regulator of JNK (Figures 2A and 2B), or of a dominant-negative form of the *JNK/basket* gene (bsk^{DN}; Figure S1). Consistently, no *en* expression was detected in these conditions (Figures 2C and 2D). In contrast, hyper-activation of JNK signaling by overexpressing *JNKK/hemipterous* (*hep*) led to an excessive number of MCs (four to five instead of two; Figures 2E, 2F, 2I, and 2J). Of note, JNK over-activation did not lead to ectopic MCs outside the A1–A5 domain, indicating that only these central segments are competent for mixing (Figures 2F and 2J). Like genuine MCs, the extra MCs also accumulate the posterior determinant En (Figures 2G and 2H).

These results show that JNK activity is specifically required in the MCs from all segments to allow their reprogramming through *en* de novo expression. However, the spatial restriction of mixing indicates that MC reprogramming is necessary but not sufficient for cell remodeling and that additional activities are required to determine the full MC phenotype.

JNK Relieves Polycomb Repression of *en* in MCs

The JNK signaling pathway is known to downregulate the expression of *Pc* during transdetermination of the regenerating imaginal discs (Lee et al., 2005). Moreover, *en* possesses PRE sequences in its promoter region that can be bound by PcG proteins (DeVido et al., 2008; Schuettengruber et al., 2009). These observations raise the interesting hypothesis that reprogramming of the MCs could depend on JNK-dependent regulation of Pc binding to *en* DNA sequences. To test this possibility, we first used qRT-PCR to analyze the expression of the *Pc* gene in JNK loss- and gain-of-function embryos (Figure 3A). No significant change in *Pc* expression was detected in *JNKK/hep* mutant embryos (JNK-LOF) using this method, likely due to limited sensitivity resulting from the small number of JNK-activated cells in each embryo (approximately only 200 LE cells in total). However, over-activation of the JNK pathway in the whole ectoderm (*69BGal4* > hep^{act}; JNK-GOF) led to the strong reduction of *Pc* expression. This result suggests that JNK signaling downregulates expression of the *Pc* gene during dorsal closure, reminiscent of what is observed during imaginal disc regeneration (Lee et al., 2005).

To further characterize *en* regulation in MCs, we next investigated the association between the *en*-PREs and the PcG bodies in the nuclei of MCs. To this goal, we used a technique coupling DNA-FISH (fluorescence in situ hybridization) to immunostaining to visualize the PcG bodies at the *en* locus (Bantignies and Cavalli, 2014) (Figure 3B). The interaction between *en*-PREs and PcG bodies was evaluated by quantifying the overlap between the Pc and *en*-PRE probe signals. The Pc signal from MCs was compared to the one of their posterior and anterior neighbors at the LE. Results show that the overlap between the *en* locus and the Pc signal is lower in posterior cells (PCs, expressing *en*) than in anterior cells (ACs, not expressing *en*) (Figure 3C; Figure S2), indicating that dissociation of Pc from the *en*-PREs is responsible for *en* expression in PCs, as shown previously (DeVido et al., 2008; Moazed and O'Farrell, 1992). Interestingly, MCs present an intermediate profile between anterior and posterior fates (Figure 3C; Figure S2), well reflecting the low level of *en* expression in the MCs compared to the strong expression seen in the PCs (Gettings et al., 2010) (Figures 1E and 1F). We then tested the effect of JNK signaling on the *en*-PREs/Pc interaction. Over-activation of JNK has no detectable effect on the *en*-PREs/Pc association, consistent with the fact that JNK is already active in MCs (Figure 3C, MC JNK-GOF). In contrast, loss of JNK activity led to an increase of the *en*-PREs/Pc association, reaching the level of the signal observed in the AC (Figure 3C, MC JNK-LOF). In this JNK-LOF condition, the anterior, repressed fate of the MC is, therefore, maintained by a high level

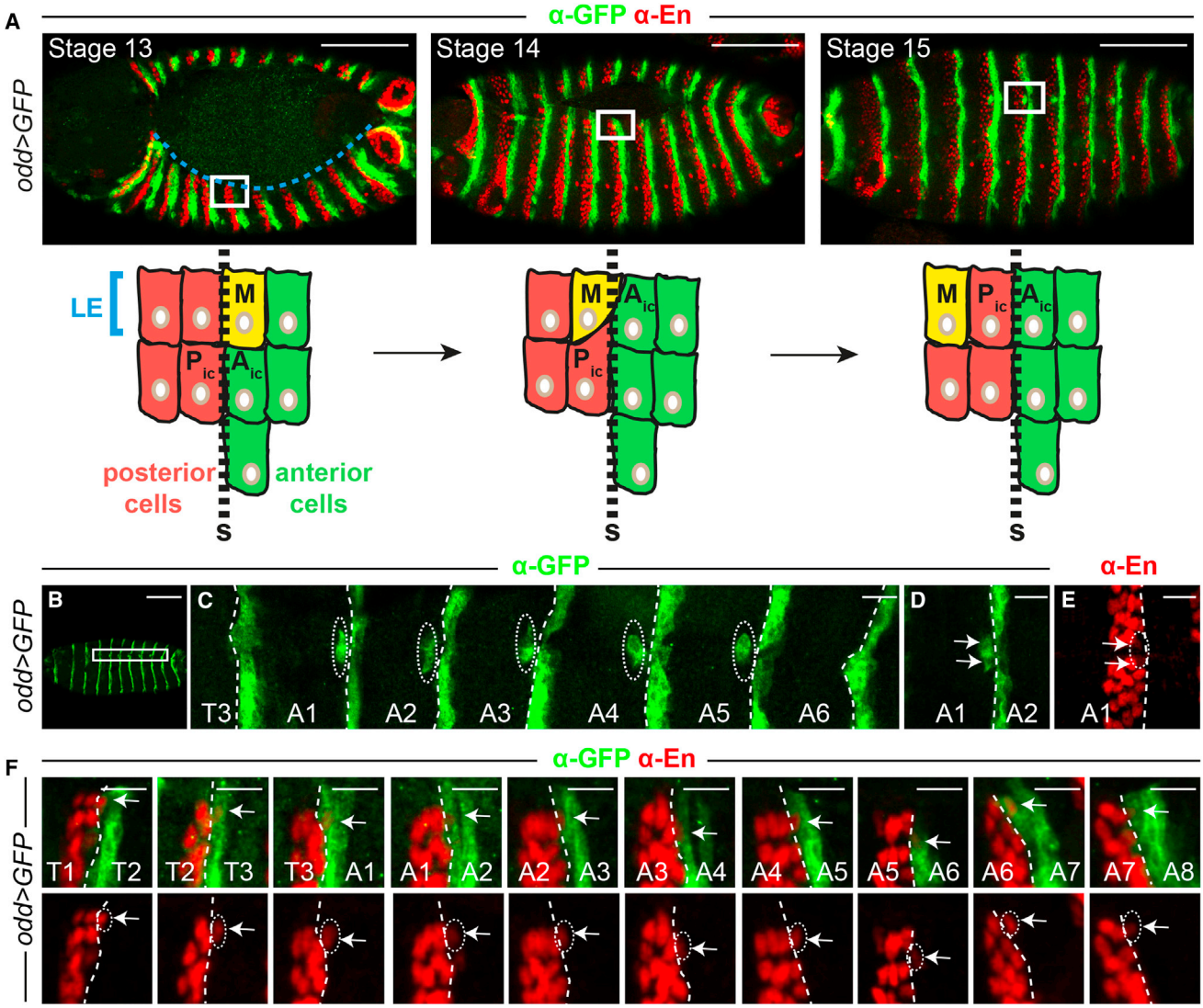

Figure 1. Reprogramming and Mixing during Dorsal Closure

(A) Fixed *odd* > *UAS-mCD8::GFP* embryos in the process of closure at stages 13, 14, and 15 stained with anti-GFP (green) and anti-En (red) antibodies. The blue dotted line delineates the leading edge (LE). The white rectangle indicates the localization of the mixing process depicted in the schematics below. At the start of dorsal closure (stage 13), the MC (M) is an AC located at the cross of the LE and the groove (left panels). As dorsal closure proceeds (stages 14–15), two cells of the row below (the posterior and anterior intercalating cells: P_{ic} and A_{ic}, respectively) integrate the LE, isolating the MC in the preceding posterior compartment (middle and right panels). The segment boundary (S) is drawn with a dotted black line.

(B) *odd* > *UAS-mCD8::GFP* embryo at the end of dorsal closure (stage 15) labeled with an anti-GFP antibody (green), in which the groove cells of each segment are GFP positive.

(C) Close-up at the dorsal midline of segments T3 to A6 (corresponding to the white box in B) showing the intercalation of MCs taking place in central segments A1 to A5 (dotted circles).

(D and E) Shown here, (D) a close-up of segments A1 and A2 showing the two GFP-positive MCs integrated and isolated in the posterior compartment (arrows) and (E) their En expression (indicated by arrows and the dotted circle).

(F) Close-up at each segment boundary (dotted line) of *odd* > *UAS-mCD8::GFP* embryos at the start of dorsal closure (stage 13) stained with anti-GFP (green) and anti-En (red) antibodies. The MCs (indicated by the arrows in the upper panels) appear as GFP-positive cells expressing the posterior determinant En (indicated by arrows and dotted circles in the bottom panels), revealing their reprogramming. Scale bars represent 100 μm for figures with the whole embryo and 10 μm for zoomed figures.

The closed dotted line in (B)–(F) outlines the cluster of mixer cells.

of *en*-PREs/Pc association. Together, these results suggest a two-repressor model (JNK represses *Pc*, which represses *en*; Figure 3D) in which MC reprogramming is due to a JNK-dependent relief of Pc inhibition at the *en* locus.

Mixing Is Abolished in *Pc* Mutant Embryos

The two-repressor model suggested earlier predicts that, in a *Pc* mutant embryo, one should observe ectopic *en* expression and mixing. As previously described (Pirrotta, 1997), and in

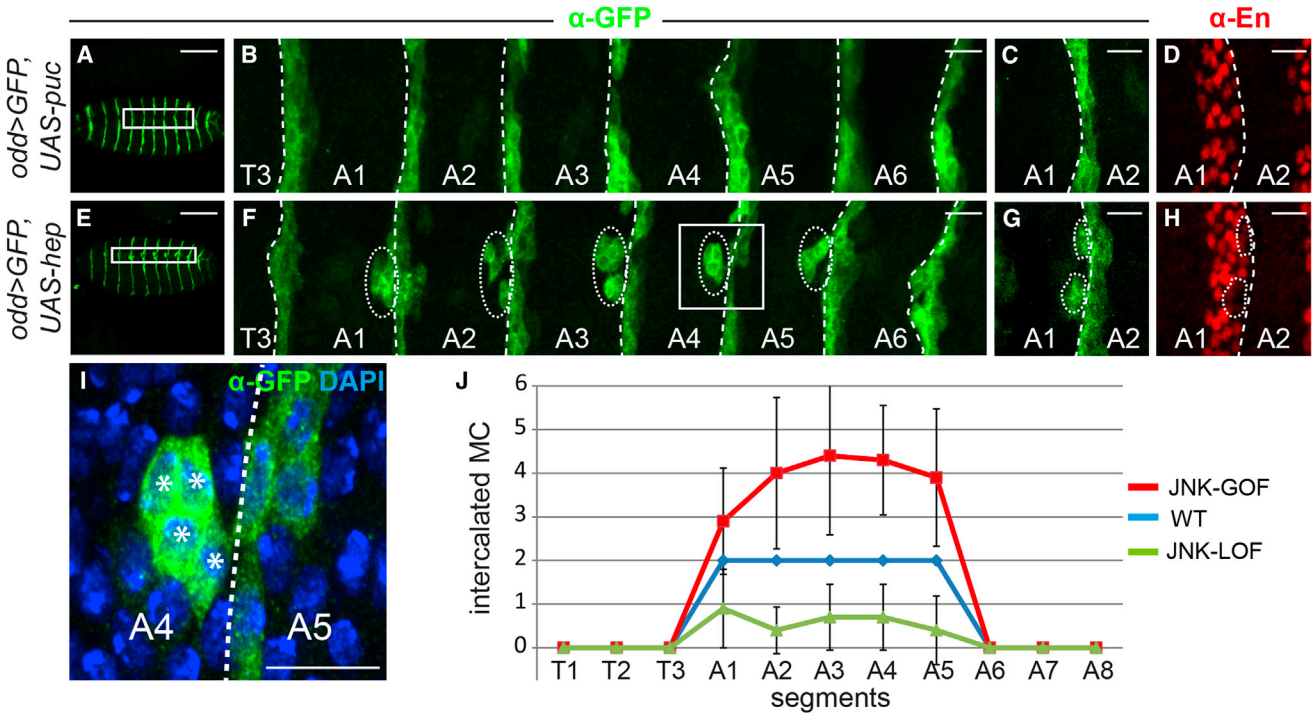

Figure 2. The JNK Signaling Pathway Controls MC Reprogramming and Mixing

(A) *odd* > *UAS-mCD8::GFP, UAS-puc* embryo stained with the anti-GFP antibody.

(B) Close-up of segments T3 to A6 (white box in A) showing the absence of mixing.

(C and D) Close-up of segments A1 and A2: MCs are absent, and no AC expressing *en* is observed.

(E) *odd* > *UAS-mCD8::GFP, UAS-hep* embryo stained with the anti-GFP antibody.

(F) Close-up of segments T3 to A6 (white box in E) showing the excessive number of MCs.

(G and H) In (G), the ectopic MCs have incorporated the posterior compartment, and (H) express *en*.

(I) Close-up of segments A4 and A5 (white box in F) showing an example of four ectopic MCs (stars).

(J) Quantification of the intercalated MCs in JNK gain-of-function (JNK-GOF) embryos (*odd* > *UAS-mCD8::GFP, UAS-hep*; n = 7) and JNK loss-of-function (JNK-LOF) embryos (*odd* > *UAS-mCD8::GFP, UAS-puc*; n = 7) compared to wild-type (WT) embryos (n = 9). The ectopic mixing triggered by the JNK-GOF is restricted to segments A1 to A5. Data are represented as mean ± SEM.

The closed dotted line outlines the cluster of mixer cells. Linear dotted lines indicate the segment boundary. See Figure 1 legend for explanation of scale bars. See also Figure S1.

agreement with our model, *en* expression expands in the anterior compartments of *Pc* mutants, especially in the lateral part of the embryo (Figures 4A and 4B). We could also observe GFP-positive cells (i.e., most ACs) which express *en*, some of them being located in the LE and thus corresponding to putative MCs (Figures 4C and 4D).

Although we observe ectopic *en* expression in the ectoderm (discussed earlier; Figures 4A–4D), we found that mixing does not occur in *Pc* embryos (Figures 4E and 4F), whose phenotype resembles that of JNK loss-of-function embryos (Figures 2A and 2B). What is the origin of this apparent discrepancy between the repressive role of Pc discussed earlier and the *Pc* phenotype?

We first controlled that *Pc* was not affecting the overall JNK activity (Figure S3). We then tested the epistatic relationship between JNK and *Pc*, suggested by our two-repressor model (Figure 3D), by analyzing mixing in *oddGal4-GFP* > hep^{act} embryos that are mutant for *Pc* (*oddGal4-GFP* > hep^{act}; *Pc*/*Pc*). In these JNK gain-of-function embryos, the supernumerary MC phenotype is clearly suppressed by loss of *Pc* (Figures 4G and 4H; compare with Figures 2E and 2F), resembling simple *Pc* mutants (Figures 4E and 4F). These results indicate that *Pc* acts downstream of, or in parallel to, JNK. Therefore, while our results confirm a role of *Pc* on *en* repression downstream of JNK (Figures 3 and 4), the *Pc* phenotype (absence of cell mixing; Figures 4E and 4F) appears more complex. To reconcile our results, we hypothesize that, in addition to *en*, Pc must be controlling another essential factor for proper MC intercalation.

As shown earlier (Figure 1), two different MC populations exist, with one population undergoing mixing (A1–A5 segments), while the other does not, despite expressing *en* (T1–T3 and A6–A7). Strikingly, the latter population resembles the MCs found in *Pc* mutants. These observations suggest a possible role of A-P cues to regulate the distribution of the different MC populations and explain the *Pc* mutant phenotype. Since *Pc* is known to regulate the Hox genes from the Bithorax complex (Lewis, 1978; Simon et al., 1993), we analyzed the expression profiles of *abdA* and *AbdB*. Whereas *abdA* is expressed from segments A1 to A7, *AbdB* expression gradually increases from A5 to the

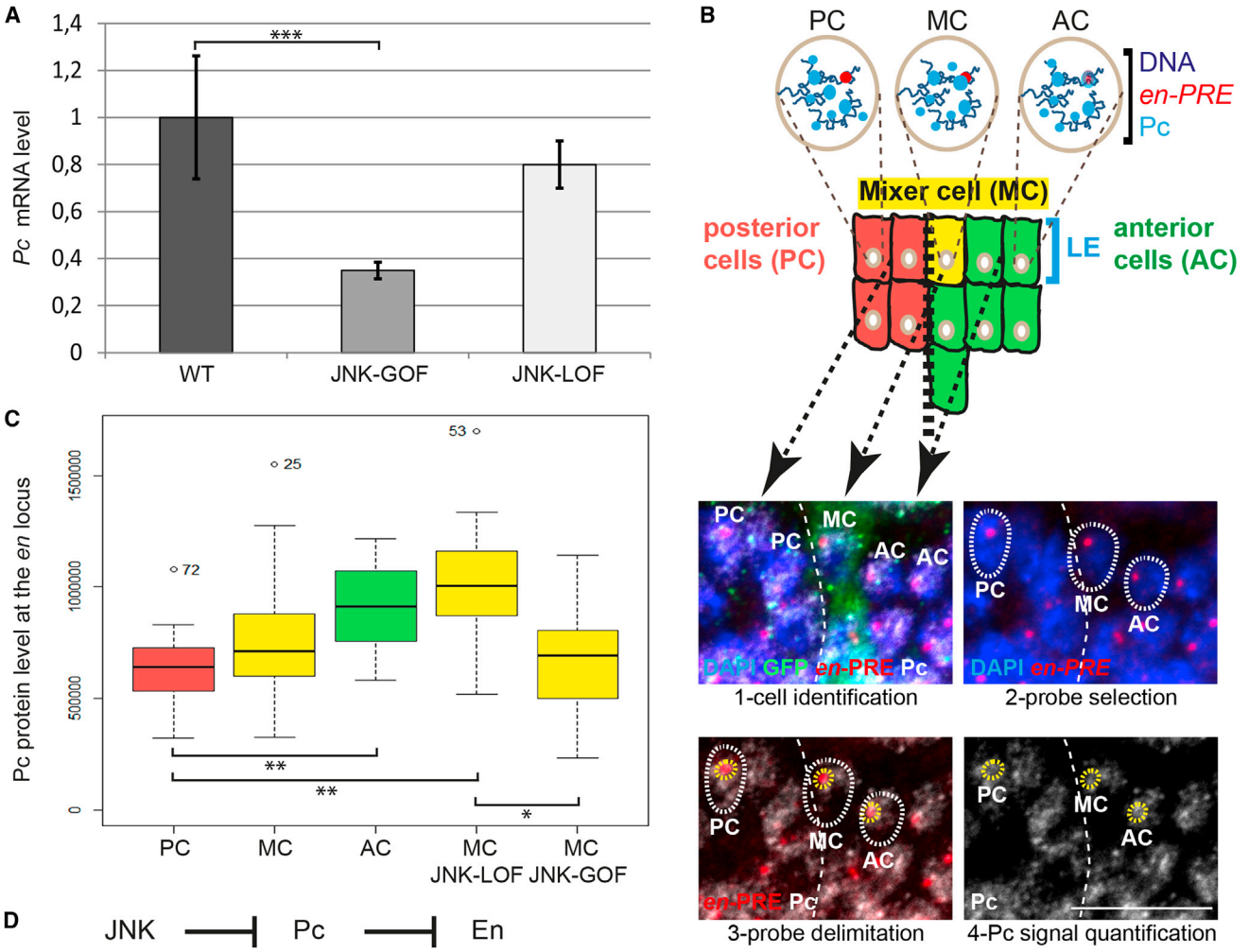

Figure 3. JNK Induces MC Reprogramming through *Pc* Repression

(A) qRT-PCR showing the negative regulation exerted by JNK on *Pc* expression. Compared to wild-type (WT) embryos (dark gray bar), the expression of *Pc* in the JNK gain-of-function condition (JNK-GOF; *69B > UAS-hep^{act}*; gray bar) is lowered. In JNK loss-of-function embryos (JNK-LOF; *hep^{r75}/hep^{1}*; light gray bar), the expected upregulation of *Pc* could not be detected, likely due to the relative small number of JNK-positive cells (the LE represents approximately 200 cells) in the whole embryo. Data are represented as mean ± SEM. ***p < 0.001.

(B) DNA-FISH experiment used to reveal the nuclear interaction between Pc and the *en* locus. The cartoon at the top schematizes the molecular mechanism of *en* repression by Pc taking place in the nucleus. In posterior cells (PCs), the *en* locus (red dot) is not included in a PcG body (blue dots), leading to the expression of *en*. In anterior cells (ACs), *en* is repressed by Pc through a strong association between Pc and the *en* locus in a PcG body. The *en* locus of the MC, an AC reprogrammed to become a posterior one, should be released by the Pc body to enable de novo expression of *en*. At the bottom, *odd > UAS-mCD8::GFP* embryos were hybridized with an *en-PRE* probe (red) to localize the *en* locus and co-stained with anti-GFP (green) and anti-Pc (white) antibodies and DAPI (blue). After cell identification using the GFP (step 1), the *en-PRE* signal was localized (step 2) and delineated (step 3). The Pc protein level was then quantified (step 4). The linear dotted line indicates segment boundary. Large closed dotted lines indicate cell nuclei. Smaller yellow dotted lines indicate the *en-PRE* probe.

(C) Boxplots showing the quantification of the Pc protein signal associated with the *en*-PREs. In control *odd > UAS-mCD8::GFP* embryos, the fluorescent intensity of Pc is higher in ACs (green; *en*-negative cells) than in PCs (red; *en*-positive cells) due to the increased localization of the *en* locus in the PcG bodies for silencing *en* expression. WT MCs (MC; yellow) present an intermediate fluorescent intensity between PCs and ACs, revealing MC reprogramming and weak de novo expression of *en*, as previously published (Gettings et al., 2010). As a control, we also quantified the Pc signal in more lateral PCs and ACs and obtained similar results (see Figure S2). In JNK loss-of-function *odd > UAS-mCD8::GFP, UAS-puc* embryos (MC JNK-LOF), the Pc fluorescent signal is higher than that of the control MC, and the LOF MCs resemble ACs. In JNK gain-of-function *odd > UAS-mCD8::GFP, UAS-hep^{act}* embryos (MC JNK-GOF), the Pc fluorescent intensity is similar to that of the control MC. *p < 0.05; **p < 0.01.

(D) The two-repressor model of the JNK-induced reprogramming of the MCs (see Results for details).

See Figure 1 legend for explanation of scale bars. See also Figure S2.

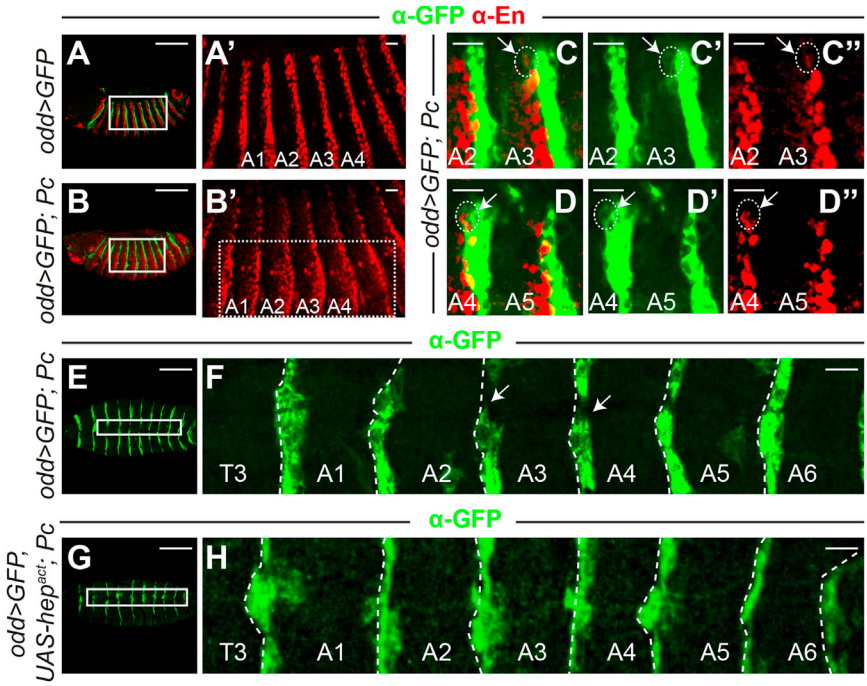

Figure 4. Mixing Is Absent in the *Pc* Mutant

(A–B') Shown here, (A) *odd* > *UAS-mCD8::GFP* embryo stained with anti-GFP and anti-En antibodies and (A') a close-up of (A) (white box) showing the expression pattern of *en*. (B) *odd* > *UAS-mCD8::GFP, Pc/Pc* embryo stained with anti-GFP and anti-En antibodies and (B') a close-up of (B) (white box) showing the expected ectopic expression of *en* (dotted rectangle), mostly visible in the lateral part of the embryo.

(C–D'') Two close-ups of dorsal regions of *odd* > *UAS-mCD8::GFP, Pc/Pc* embryos showing anterior GFP-positive cells (green, indicated by the arrows and dotted lines) also expressing *en* (red), indicating that, even though there is no mixing, MC reprogramming occurs in the *Pc* mutant. Overlay (C and D); GFP (C' and D'); En (C'' and D'').

(E) *odd* > *UAS-mCD8::GFP, Pc/Pc* embryo stained with the anti-GFP antibody.

(F) Close-up of segments T3 to A6 (white box in E) showing the absence of mixing. Occasionally, we could observe an absence of GFP-positive cells at the dorsal midline once dorsal closure is accomplished (arrows). Linear dotted lines indicate the segment boundary.

(G) *odd* > *UAS-mCD8::GFP, UAS-hep^{act}, Pc/Pc* embryo stained with the anti-GFP antibody.

(H) Close-up of segments A1 to A6 (white box in G) in which only few MCs integrate into the posterior compartments, indicating that *Pc* is required for JNK-dependent mixing. Linear dotted lines indicate the segment boundary.

See Figure 1 legend for explanation of scale bars. See also Figure S3.

end of the embryo (Figures 5A–5D), as previously shown (Simon et al., 1992). Therefore, mixing specifically takes place in the *abdA* territory, where no or very weak expression of *AbdB* is detected, suggesting that *abdA* could be an important activator in the process while *AbdB* could be acting as an inhibitor. In the *Pc* mutant embryo, *abdA* expression expands anteriorly while being maintained in segments A1 to A7 (Figures 5E and 5F) (Simon et al., 1992). Similarly, *AbdB* is ectopically expressed in the whole anterior of the *Pc* mutant (Figures 5G and 5H) (Simon et al., 1992). Therefore, in *Pc* mutant embryos, both *abdA* and *AbdB* are co-expressed along the whole A-P axis, with *AbdB* ectopic expression possibly causing the absence of mixing in these embryos.

abdA and *AbdB* Spatially Control Mixing during Dorsal Closure

To analyze the role of *abdA* and *AbdB* on mixing, we first examined the phenotype of loss-of-function mutants. Integration of the MCs was assessed by immunostaining against the groove-cell marker Enabled (Ena), a cytoskeleton protein overexpressed in *odd*-positive cells (the groove cells) and the LE (Gates et al., 2007). At the end of dorsal closure, MCs can thus be identified as Ena-positive cells in the posterior compartments that also express En (Figures 6A–6C) (Gettings et al., 2010). In *abdA* mutant embryos, mixing is strongly reduced (Figure 6D). Although MCs form correctly, with a normal *en* expression, they show incomplete mixing in the *abdA* mutant, with MCs staying attached to the groove (Figures 6E and 6F). These results indicate that, although *abdA* is not essential for MC transdifferentiation, it positively regulates MC integration into the posterior compartment, suggesting a role in the mixing process itself. In *AbdB* mutant embryos, mixing spreads posteriorly and can now be detected in segments A6 and A7 in 100% of the embryos, with MCs normally expressing *en* (Figures 6G–6I). Mixing is never observed in this region in wild-type (WT) embryos (Figures 1B, 1C, and 2J). These results indicate that *AbdB* is a major repressor of mixing and that *abdA* and *AbdB* have antagonistic functions. In segments where both *abdA* and *AbdB* are expressed (i.e., A6 and A7), mixing does not occur. This reveals that the negative action of *AbdB* is prevalent over *abdA*, reflecting the well-known posterior dominance of the Hox genes. In support of this view, co-expression of both Hox genes led to a strong reduction of mixing, like in the *Pc* mutant (Figure 6J).

To further establish the role of *abdA* and *AbdB* in MCs, these genes were individually overexpressed in MCs using the *oddGal4-GFP* driver. AbdA overexpression is sufficient to induce ectopic mixing more anteriorly, as observed in the T1, T2, and T3 segments (Figures 6K–6M). In contrast, mixing is abolished in all segments upon AbdB overexpression (Figures 6N–6P). Similar results were obtained using the *patched* (*ptc*) *Gal4-GFP* driver, which is expressed in the whole anterior compartment (Figure S4). These results confirm the loss-of-function data and indicate that *abdA* is a general positive regulator of mixing, while *AbdB* behaves as a strong prevalent repressor. The *oddGal4* > *abdA* experiment indicates that *abdA* may promote mixing by acting in the MC itself or in the groove cell located more laterally. To distinguish between these two possibilities, *abdA* was overexpressed in the LE using the *LE-Gal4* driver, leading to mixing

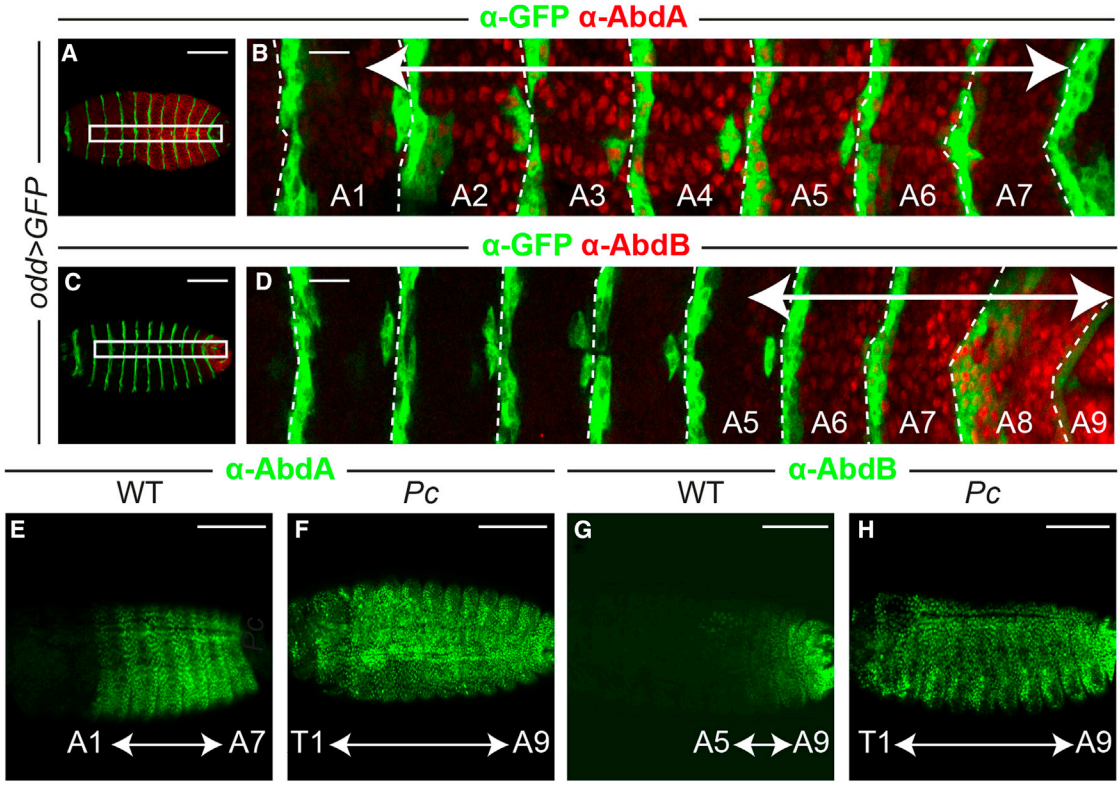

Figure 5. *abdA* and *AbdB* Expression in WT and *Pc* Embryos

(A) *odd* > *UAS-mCD8::GFP* embryos stained with anti-GFP and anti-AbdA antibodies to analyze the expression profile of *abdA*.

(B) Close-up of segments A1 to A7 (white box in A) showing that AbdA expression (red) is observed from the posterior compartment of the A1 segment to the A7 segment. Linear dotted lines indicate the segment boundary.

(C) *odd* > *UAS-mCD8::GFP* embryo stained with anti-GFP and anti-AbdB antibodies showing the expression profile of *AbdB*.

(D) Close-up of segments A1 to A9 (white box in C) showing that AbdB expression (red) spreads from the posterior compartment of the A5 (weak expression) through the end of the embryo (strongest expression). Linear dotted lines indicate the segment boundary.

(E) WT expression of AbdA (anti-AbdA staining) in segments A1 to A7.

(F–H) Shown in (G) is the WT expression of AbdB (anti-AbdB staining) in segments A5 to A9. (F and H) In the *Pc* mutant embryo, the two Hox genes *abdA* (F) and *AbdB* (H) are ectopically misexpressed all along the A-P axis.

See Figure 1 legend for explanation of scale bars.

in the T3 segment and thus showing that the action of *abdA* takes place specifically in the MC (Figures 6Q and 6R).

We then analyzed the epistatic relationship between *abdA* and JNK signaling. Overexpression of *abdA* was not sufficient to induce mixing in JNK loss-of-function embryos (Figures 7A and 7B; compare with *oddGal4-GFP* > *puc* embryos in Figures 2A and 2B), indicating that JNK-induced MC transdifferentiation is required for AbdA-dependent cell mixing. As a control, we have verified that AbdA itself is not capable of turning on *en* de novo expression (Figure S5). In contrast, *abdA* overexpression in the JNK gain-of-function condition induced ectopic mixing in the most anterior T2 and T3 compartments, as observed in embryos overexpressing *abdA* (Figures 7C and 7D; compare with Figure 6K). These results are consistent with the fact that the JNK gain of function does not change the *en*-PRE/Pc association, reflecting a fully activated pathway in WT embryos (Figure 3C). Therefore, JNK and *abdA* are both required to trigger cell mixing by regulating transdifferentiation of MCs and cell remodeling, respectively.

Altogether, our results identify a gene regulatory network involving a two-tiered role of *Pc*, negatively regulating *en* expression and MC reprogramming on the one hand and positively activating mixing through *abdA* and *AbdB* gene regulation on the other hand. Interestingly, this model provides a solution to the paradoxical phenotype of the *Pc* mutant, in which mixing was not observed. In this condition, AbdA and AbdB are ectopically co-expressed along the A-P axis (Figure 5), but since AbdB has a prevalent negative role on AbdA, MCs cannot mix and cross the segment boundary.

DISCUSSION

Our previous work showed that transdifferentiation of MCs during dorsal closure requires JNK-dependent de novo expression of the *en* posterior determinant (Gettings et al., 2010). This developmental reprogramming process leads to plasticity of the segment boundary through direct lineage switching. Here, we reveal a two-tiered role of *Pc* and chromatin remodeling in

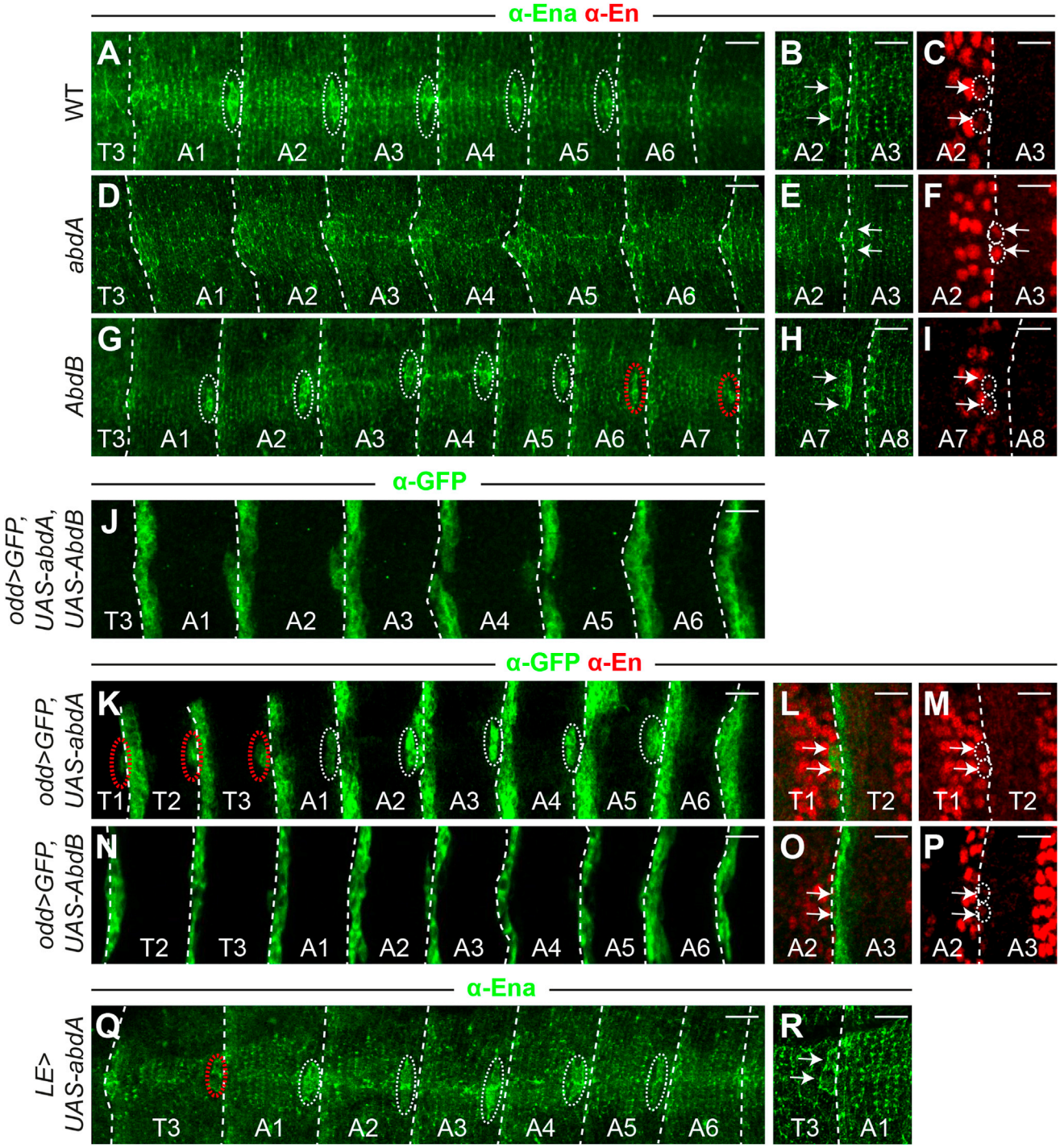

Figure 6. Regulation of Mixing by the Hox Genes *abdA* and *AbdB*

(A) Segments T3 to A6 of a WT embryo stained with an anti-Ena antibody (green; groove cell marker) showing MCs, coming from the groove, which have mixed (dotted circles) in segments A1 to A5.

(B and C) Shown here, (B) a close-up of segments A2 and A3 in (A) showing MC intercalation (indicated by the arrows) and (C) their *en* expression (indicated by dotted circles).

(D) Segments T3 to A6 of the *abdA* mutant showing the absence of mixing.

(E and F) Shown here, (E) a close-up of segments A2 and A3 showing MCs staying attached to the anterior groove cells (arrows) and (F) their *en* expression (dotted circles).

(G) Segments T3 to A7 of the *AbdB* mutant embryo showing ectopic mixing in the posterior segments A6 and A7 (red dotted circles).

(legend continued on next page)

regulating the pattern of MC formation (Figure 7E). First, we show that the association between the *en* locus and the PcG bodies is tightly linked to *en* expression and JNK activity. Our results reveal a model in which JNK downregulates the expression of *Pc*, thereby releasing its negative activity on the *en* promoter. Second, we show that regulation of Hox gene activity by Pc controls the spatial pattern of MC formation along the A-P axis. In this process, *abdA* functions as a positive mixing factor, allowing MCs to cross the segment boundary, while *AbdB* behaves as a strong repressor of mixing. Thus, crosstalk between JNK, *Pc*, *en*, and Hox function controls the pattern of MC formation and their mixing in A1–A5 segments specifically (Figure 7E).

Mixing along the A-P axis can be separated in three distinct domains and can be linked to the activity of AbdA and AbdB. In the posterior segments (A6 and A7), both AbdA and AbdB are expressed, but mixing does not occur due to the prevalent, negative role of AbdB. This effect reflects the well-known phenomenon of Hox posterior prevalence, in which posterior Hox genes dominate the activity of more anterior ones (Duboule and Morata, 1994). In the central abdominal segments (A1 to A5), Pc specifically represses the expression of AbdB, and the activity of the pro-mixing factor AbdA promotes mixing. In the thoracic segments (T1–T3), AbdA is normally repressed by Pc; therefore, mixing does not occur. Altogether, our results indicate that transdifferentiation and mixing are two separate and sequential components of the MC phenotype: first, transdifferentiation takes place in all MCs (from T1–A7 segments), due to JNK-dependent relief of Pc repression of the *en* promoter; de novo expression of *en* makes MCs competent for mixing proper. Second, the pattern of mixing along the A-P axis depends on the activity of Hox genes (*abdA* and *AbdB*), with *abdA* playing a key pro-mixing activity (Figure 7E).

We previously proposed two potential roles for the mixing process during dorsal closure (Gettings and Noselli, 2011; Gettings et al., 2010). In a first scenario, mixing could contribute to the perfect matching of contralateral segments, since one striking consequence of mixing is to generate cell diversity at the segment boundary along the LE by alternating distinct cell fates (Gettings et al., 2010). This view was supported by the fact that loss of JNK activity in the anterior compartment (using the *ptcGal4* driver) led to segment mismatches (Gettings et al., 2010). However, we did not observe any segmental mismatch when we inhibited JNK (and thus mixing) only in the groove cells using *oddGal4* (Figures 2A and 2B), suggesting that mixing might not be directly involved in segment alignment. A second possible role of mixing is to release tension thanks to the integration of supernumerary cells into the LE through cell intercalation. Laser ablation experiments showed accordingly that mixing is slowed down when tension is released (Gettings et al., 2010). Tension has been shown to increase with closure (Hutson et al., 2003; Kiehart et al., 2000), and the central segments, which close last, are thus subject to increasing tension during dorsal closure. Thus, mixing responds to tension and takes place in the region of highest tension. These observations support a model in which the MCs serve as a sensor of tissue tension triggering cell intercalation and, hence, tension release.

Our work reveals another important role of JNK during dorsal closure, in addition to its well-known role in controlling LE gene expression and tissue sealing. JNK can, indeed, induce transdifferentiation in the MCs, resulting in segment boundary remodeling. As such, JNK signaling generates plasticity in patterning through nuclear reprogramming and crosstalk with PcG genes. How general is this role during *Drosophila* development? Interestingly, transdetermination, collapse of the segment boundary, and mixing of ACs and PCs have also been reported during regeneration of imaginal discs (Herrera and Morata, 2014). When wounding is done at specific regions named weak points, the frequency of reprogramming is enhanced (Gehring et al., 1968). Similarly, we could consider the MCs as weak points, similar to micro-wounds that can trigger LE repair through cell intercalation at the segment boundary (Gettings et al., 2010). In the imaginal disc, ablation near the A-P boundary leads ACs to mix in the posterior compartment and vice versa (Morata and Lawrence, 1975). At sites of regeneration, the JNK signaling pathway is activated to downregulate *Pc* (Herrera and Morata, 2014; Lee et al., 2005; Morata and Lawrence, 1975), thus favoring chromatin remodeling and subsequent transdetermination. We showed that the same mechanism occurs in the MCs, suggesting that regeneration may be an instance in which a developmental reprogramming event (MC) is re-used upon injury in the imaginal discs. Therefore, deciphering the mechanisms controlling MC transdifferentiation may help us better understand those involved during reprogramming at regeneration sites.

EXPERIMENTAL PROCEDURES

Fly Stocks and Handling

w^{1118} (Bloomington Drosophila Stock Center [BDSC] #3605) was used as a WT fly. Mutants strains used in this study are the following: hep^{r75} and hep^{1} (Glise et al., 1995), Pc^{XT109} (BDSC #24468), $abdA^{M1}$ (Struhl and White, 1985), and $AbdB^{D18}$ (Hopmann et al., 1995). The following *UAS* and *Gal4* lines have been used: *UAS-mCD8::GFP* (BDSC #5137), *UAS-hep* (*UAS-hep*^{4E}) (Glise et al., 1995), *UAS-hep*^{act} (BDSC #9306), *UAS-bskDN* (BDSC #9311),

(H and I) Shown here, (H) a close-up of segments A7 and A8 showing the ectopic MCs (arrows) and (I) their *en* expression (dotted circles).
(J) Segments T3 to A6 of an *odd* > *UAS-mCD8::GFP, UAS-AbdB, UAS-abdA* embryo showing a strong diminution of mixing (phenotype similar to the *Pc* mutant phenotype) and revealing the dominance of *AbdB* (negative regulator) on *abdA* (positive regulator).
(K) Segments T1 to A6 of an *odd* > *UAS-mCD8::GFP, UAS-abdA* embryo showing ectopic mixing in the thoracic segments T1 to T3 (red dotted circles).
(L and M) Shown here, (L) a close-up of segments T1 and T2 showing MC intercalation and (M) their *en* expression.
(N) Segments T1 to A6 of an *odd* > *UAS-mCD8::GFP, UAS-AbdB* embryo showing the inhibition of mixing.
(O and P) Shown here, (O) a close-up of segments A2 and A3 showing the MCs and (P) their *en* expression.
(Q) Segments T3 to A6 of an *LE* > *UAS-abdA* embryo stained with the anti-Ena antibody showing ectopic mixing in T3 (red dotted circle), thus indicating that *abdA* promotes mixing by acting in the MC.
(R) Close-up of segments T3 and A1 showing the mixing of the two MCs.
The closed dotted line outlines the cluster of mixer cells. Linear dotted liens indicate the segment boundary. See Figure 1 legend for explanation of scale bars. See also Figure S4.

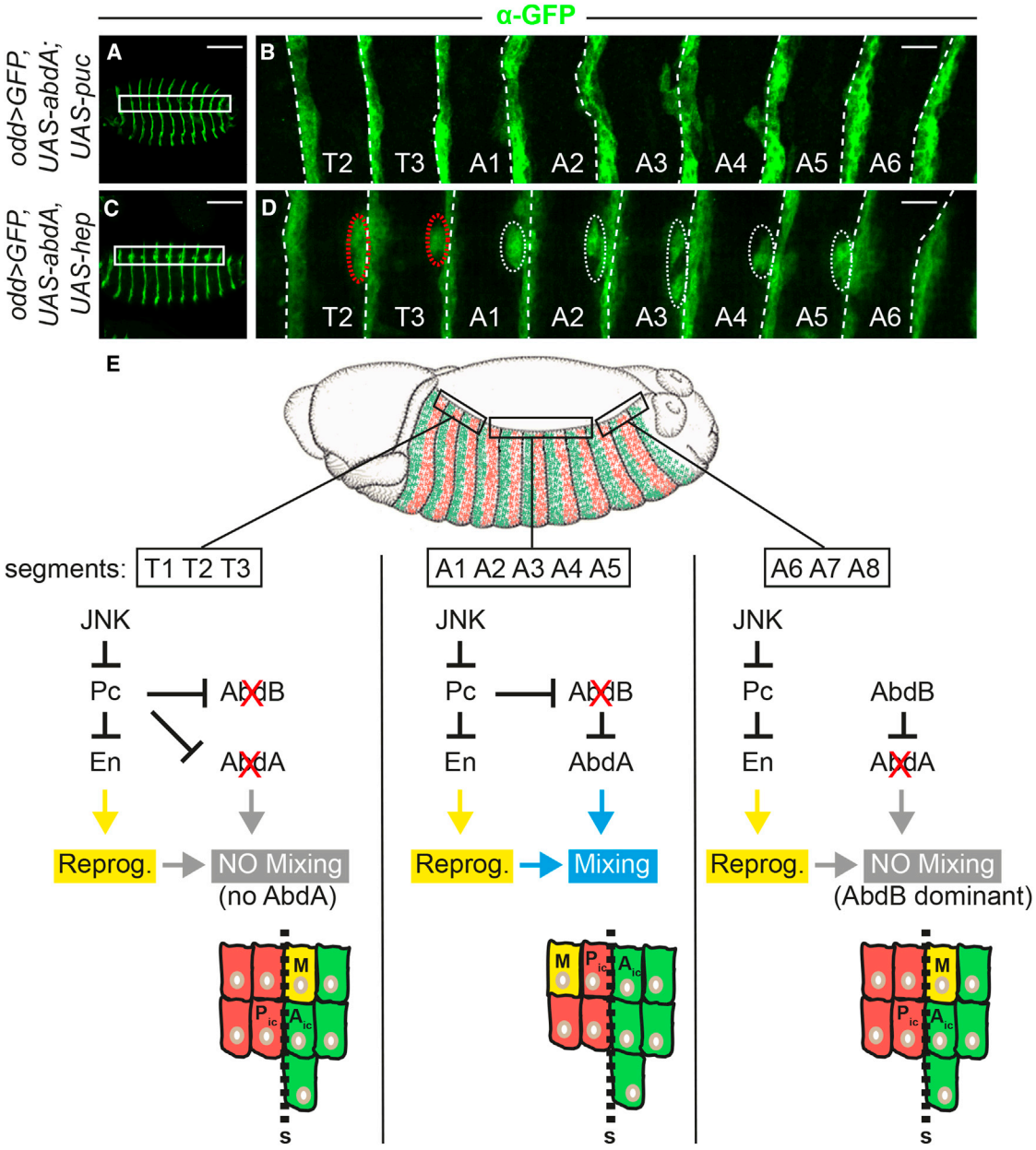

Figure 7. JNK, *Pc*, and Hox Regulation of Mixing

(A) *odd* > *UAS-mCD8::GFP, UAS-puc, UAS-abdA* embryo stained with the anti-GFP antibody.

(B) Close-up of segments T2 to A6 (white box in A) showing the almost total absence of mixing.

(C) *odd* > *UAS-mCD8::GFP, UAS-hep, UAS-abdA* embryo stained with the anti-GFP antibody.

(D) Close-up of segments T2 to A6 (white box of C) showing the excessive number of MCs produced in anterior segments T2 and T3 (red dotted circles). The closed dotted line outlines the cluster of mixer cells.

(E) Model of MC reprogramming (Reprog.) and mixing along the A-P axis of the embryo (see Discussion for details). M, MCs; S, segment boundary.

In (B) and (D), linear dotted lines indicate the segment boundary.See Figure 1 legend for explanation of scale bars. See also Figure S5.

UAS-puc (Martín-Blanco et al., 1998), *UAS-abdA::HA* and *UAS-AbdB::HA* (Banreti et al., 2014), *LE-Gal4* (BDSC #58801), *oddGal4* (provided by L.S. Shashidhara), *69BGal4* (BDSC #1774), and *ptcGal4* (provided by N. Perrimon). The strains w^{-}*; oddGal4, UAS-mCD8::GFP* and w^{-}*; ptcGal4, UAS-mCD8::GFP* have been constructed by recombination. For crosses, flies were raised at 25°C or 29°C, and embryos were collected after 14- to 15-hr overnight incubations.

Antibody Staining and RNA-FISH of Whole-Mount Embryos

Embryos were devitellinized in bleach, fixed in 4% formaldehyde, and dechorionated in heptane/methanol. Fixed embryos were blocked for 2 hr in PBS-Tween 0.1% and BSA 1%. To improve staining of En and Ena, this step was omitted. Embryos were then incubated for 2 hr or overnight in PBS-Tween 0.1% with the following primary antibodies: goat anti-GFP (1:500, Rockland), rabbit-anti-Pc (1:500, gift from F. Bantignies), rabbit anti-En (1:400, Santa

Cruz Biotechnology), mouse anti-Ena (1:100, Developmental Studies Hybridoma Bank [DSHB]), mouse anti-AbdA (1:200, DSHB), mouse anti-AbdB (1:200, DSHB), and rat anti-HA (anti-hemagglutinin) (1/500, Sigma-Aldrich). After six 10-min washes in PBS-Tween 0.1%, embryos were incubated for 2 hr with purified secondary antibodies: Alexa Fluor 488, Alexa Fluor 546, and Alexa Fluor 647 (1:200, Molecular Probes). In some cases for the En staining, the signal was amplified by coupling the secondary anti-rabbit-HRP (horseradish peroxidase) (1:200, GE Healthcare) to the TSA Cyanine Plus kit (PerkinElmer LAS). After six 10-min washes in PBS-Tween 0.1%, DAPI solution (1:1,000 of a 10 μg/mL solution; Biochemika) was used to stain nuclei. Stained embryos were mounted in Mowiol 4-88 (Calbiochem) for further observation under an LSM 780 Zeiss confocal microscope. Mutant embryos were discriminated from control embryos by specific antibody stainings. RNA-FISH was performed as described (Rousset et al., 2010).

qPCR

Total RNA was extracted from frozen embryos, lysed in RLT Buffer + β-mercaptoethanol 2× for 30 s at 30 rpm/s, and purified (QIAGEN RNeasy Mini Kit). Reverse transcription was performed with SuperScript III Reverse Transcriptase (Invitrogen Life Technology) after DNase I digestion with a mix of oligo-dT and random primers. Gene-specific primers were designed with the Primer Express software (Applied Biosystems) and tested. qPCR was performed with the Mastermix Plus for SYBR Green containing Rox (Eurogentec) with the endogenous *RpL32* (*rp49*) gene for normalization. The list of primers that were used is available upon request. Standard curves of all the couples of primers presented an efficacy of amplification between 95% and 110%, with a coefficient of determination, R^2, of at least 0.995. For each condition, we did three biological and three technical replicates. Results were analyzed with the StepOne software v.2.1 (Applied Biosystems). The thermal cycling conditions were composed of 50°C for 2 min followed by an initial denaturation step at 95°C for 10 min, 45 cycles at 95°C for 30 s, 60°C for 30 s, and 72°C for 30 s. The relative quantification in gene expression was determined using the 2-ΔΔCt method. Using this method, we obtained the fold changes in gene expression normalized to the internal control gene (*RpL32*). Statistical analysis between WT, JNK-GOF, and JNK-LOF conditions was performed using the Dunnett test (nonparametric multiple comparison to the WT control).

DNA-FISH Coupled to Immunostaining

For the *en* locus, six overlapping genomic PCR fragments of 2 kb, covering 12 kb of the promoter region, were pooled for probe labeling. Probes were labeled using the FISH Tag DNA Multicolor Kit (Invitrogen) according to the manufacturer's instructions. DNA-FISH on whole-mount embryos was performed as previously described (Bantignies and Cavalli, 2014). After post-hybridization washes, embryos were blocked in PBSTr (PBS, 0.3% Triton), 1% BSA for 2 hr at room temperature and incubated overnight at 4°C in PBSTr/3% BSA with the rabbit anti-Pc antibody (1:250, kindly supplied by F. Bantignies). Embryos were then washed several times in PBSTr, blocked again in PBSTr/1% BSA for 1 hr at room temperature, and incubated sequentially in blocking buffer with the anti-rabbit Alexa Fluor 647 (1:200, Molecular Probes) for 1 hr at room temperature. DNA was counterstained with DAPI, and embryos were mounted in Mowiol 4-88 (Calbiochem). Images were acquired with a Zeiss LSM 780 microscope, with a 63× Plan/Apo objective (NA, 1.4). For each color channel, z stacks of 6–7 μm were collected at 0.5-μm intervals along the z axis (i.e., 13–15 slices per stack) with the Zeiss software. Three-dimensional (3D) stacks of raw images were reconstituted for each channel and color combined to give multichannel 3D stacks with the ImageJ software. The interaction of *en*-PRE with PcG bodies was evaluated in terms of fluorescent intensity of the Pc signal at the region of the *en*-PRE probe signal. First, we identified the cell type (ACs, MCs, or PCs). Once identified, we selected the probe signal area to measure the fluorescent intensity of the Pc signal in that region. If several PCs or ACs were selected on one image, the median was calculated. Quantification was performed on 15 images for the WT condition, 14 for the JNK-GOF condition, 12 for the JNK-LOF condition, and 11 for the lateral PCs/ACs. For the statistical analysis, we performed, with the R software, pairwise comparisons using nonparametric permutational t tests (method = false discovery rate [FDR]; Monte Carlo resampling = 10,000).

SUPPLEMENTAL INFORMATION

Supplemental Information includes five figures and can be found with this article online at http://dx.doi.org/10.1016/j.celrep.2017.03.033.

AUTHOR CONTRIBUTIONS

Conceptualization, S.R., R.R., and S.N.; Formal Analysis, R.R.; Methodology, S.R., R.R., and S.N.; Investigation, S.R. and R.R.; Project Administration, R.R. and S.N.; Resources, S.R. and R.R.; Supervision, R.R. and S.N.; Validation, S.R., R.R., and S.N.; Visualization, S.R., R.R., and S.N.; Funding Acquisition, R.R. and S.N.; Writing –Original Draft, S.R., R.R., and S.N.; Writing – Review & Editing, R.R. and S.N.

ACKNOWLEDGMENTS

We wish to thank E. Sanchez-Herrero, Y. Graba, F. Bantignies, L.S. Shashidhara, N. Perrimon, R. Delanoue, the Bloomington Drosophila Stock Center (BDSC), and the Developmental Studies Hybridoma Bank (DSHB) for fly stocks and reagents. We are fully grateful to F. Bantignies for giving us the opportunity to learn the DNA-FISH technique in his laboratory. We thank D. Cérézo for technical assistance and all members of the S.N. laboratory, F. Bantignies, and S. Merabet for insightful discussions. We acknowledge the imagery platform PRISM of our institute for their assistance. This work is supported by the Centre National de la Recherche Scientifique, the Agence Nationale de la Recherche (program ANR-11-BSV2-0022 - JNKDro), and LABEX SIGNALIFE (#ANR-11-LABX-0028-01). S.R. was supported by grants of the Ministère de l'Enseignement Supérieur et de la Recherche Scientifique, the Fondation pour la Recherche Médicale (fellowship code FDT20140930827), and the Cancéropôle PACA.

Received: November 2, 2016
Revised: February 3, 2017
Accepted: March 9, 2017
Published: April 4, 2017

REFERENCES

Agnès, F., and Noselli, S. (1999). [Dorsal closure in Drosophila. A genetic model for wound healing?]. C. R. Acad. Sci. III *322*, 5–13.

Banreti, A., Hudry, B., Sass, M., Saurin, A.J., and Graba, Y. (2014). Hox proteins mediate developmental and environmental control of autophagy. Dev. Cell *28*, 56–69.

Bantignies, F., and Cavalli, G. (2006). Cellular memory and dynamic regulation of polycomb group proteins. Curr. Opin. Cell Biol. *18*, 275–283.

Bantignies, F., and Cavalli, G. (2011). Polycomb group proteins: repression in 3D. Trends Genet. *27*, 454–464.

Bantignies, F., and Cavalli, G. (2014). Topological organization of Drosophila Hox genes using DNA fluorescent in situ hybridization. Methods Mol. Biol. *1196*, 103–120.

DeVido, S.K., Kwon, D., Brown, J.L., and Kassis, J.A. (2008). The role of Polycomb-group response elements in regulation of *engrailed* transcription in *Drosophila*. Development *135*, 669–676.

DiNardo, S., Sher, E., Heemskerk-Jongens, J., Kassis, J.A., and O'Farrell, P.H. (1988). Two-tiered regulation of spatially patterned *engrailed* gene expression during *Drosophila* embryogenesis. Nature *332*, 604–609.

Duboule, D., and Morata, G. (1994). Colinearity and functional hierarchy among genes of the homeotic complexes. Trends Genet. *10*, 358–364.

Gates, J., Mahaffey, J.P., Rogers, S.L., Emerson, M., Rogers, E.M., Sottile, S.L., Van Vactor, D., Gertler, F.B., and Peifer, M. (2007). Enabled plays key roles in embryonic epithelial morphogenesis in *Drosophila*. Development *134*, 2027–2039.

Gehring, W., Mindek, G., and Hadorn, E. (1968). Auto- und allotypische Differenzierungen aus Blastemen der Halterenscheibe von *Drosophila melanogaster* nach Kultur in vivo [Auto- and allotypical differentiation of the haltere disc

blastemata of Drosophila melanogaster after culture in vivo]. J. Embryol. Exp. Morphol. *20*, 307–318.

Geisler, S.J., and Paro, R. (2015). Trithorax and Polycomb group-dependent regulation: a tale of opposing activities. Development *142*, 2876–2887.

Gettings, M., and Noselli, S. (2011). Mixer Cell formation during dorsal closure: a new developmental model of JNK-dependent natural cell reprogramming in Drosophila. Fly (Austin) *5*, 327–332.

Gettings, M., Serman, F., Rousset, R., Bagnerini, P., Almeida, L., and Noselli, S. (2010). JNK signalling controls remodelling of the segment boundary through cell reprogramming during Drosophila morphogenesis. PLoS Biol. *8*, e1000390.

Glise, B., Bourbon, H., and Noselli, S. (1995). *hemipterous* encodes a novel Drosophila MAP kinase kinase, required for epithelial cell sheet movement. Cell *83*, 451–461.

Graf, T. (2011). Historical origins of transdifferentiation and reprogramming. Cell Stem Cell *9*, 504–516.

Graf, T., and Enver, T. (2009). Forcing cells to change lineages. Nature *462*, 587–594.

Herrera, S.C., and Morata, G. (2014). Transgressions of compartment boundaries and cell reprogramming during regeneration in *Drosophila*. eLife *3*, e01831.

Hopmann, R., Duncan, D., and Duncan, I. (1995). Transvection in the iab-5,6,7 region of the bithorax complex of Drosophila: homology independent interactions in trans. Genetics *139*, 815–833.

Hutson, M.S., Tokutake, Y., Chang, M.S., Bloor, J.W., Venakides, S., Kiehart, D.P., and Edwards, G.S. (2003). Forces for morphogenesis investigated with laser microsurgery and quantitative modeling. Science *300*, 145–149.

Jarriault, S., Schwab, Y., and Greenwald, I. (2008). A *Caenorhabditis elegans* model for epithelial-neuronal transdifferentiation. Proc. Natl. Acad. Sci. USA *105*, 3790–3795.

Jung, J., Zheng, M., Goldfarb, M., and Zaret, K.S. (1999). Initiation of mammalian liver development from endoderm by fibroblast growth factors. Science *284*, 1998–2003.

Kiehart, D.P., Galbraith, C.G., Edwards, K.A., Rickoll, W.L., and Montague, R.A. (2000). Multiple forces contribute to cell sheet morphogenesis for dorsal closure in Drosophila. J. Cell Biol. *149*, 471–490.

Larsen, C.W., Hirst, E., Alexandre, C., and Vincent, J.P. (2003). Segment boundary formation in Drosophila embryos. Development *130*, 5625–5635.

Lee, N., Maurange, C., Ringrose, L., and Paro, R. (2005). Suppression of Polycomb group proteins by JNK signalling induces transdetermination in *Drosophila* imaginal discs. Nature *438*, 234–237.

Lewis, E.B. (1978). A gene complex controlling segmentation in Drosophila. Nature *276*, 565–570.

Martín-Blanco, E., Gampel, A., Ring, J., Virdee, K., Kirov, N., Tolkovsky, A.M., and Martinez-Arias, A. (1998). *puckered* encodes a phosphatase that mediates a feedback loop regulating JNK activity during dorsal closure in *Drosophila*. Genes Dev. *12*, 557–570.

Moazed, D., and O'Farrell, P.H. (1992). Maintenance of the *engrailed* expression pattern by *Polycomb* group genes in *Drosophila*. Development *116*, 805–810.

Morata, G., and Lawrence, P.A. (1975). Control of compartment development by the engrailed gene in Drosophila. Nature *255*, 614–617.

Mulinari, S., and Häcker, U. (2009). Hedgehog, but not Odd skipped, induces segmental grooves in the *Drosophila* epidermis. Development *136*, 3875–3880.

Noselli, S. (1998). JNK signaling and morphogenesis in Drosophila. Trends Genet. *14*, 33–38.

Pirrotta, V. (1997). Chromatin-silencing mechanisms in *Drosophila* maintain patterns of gene expression. Trends Genet. *13*, 314–318.

Red-Horse, K., Ueno, H., Weissman, I.L., and Krasnow, M.A. (2010). Coronary arteries form by developmental reprogramming of venous cells. Nature *464*, 549–553.

Rousset, R., Bono-Lauriol, S., Gettings, M., Suzanne, M., Spéder, P., and Noselli, S. (2010). The *Drosophila* serine protease homologue Scarface regulates JNK signalling in a negative-feedback loop during epithelial morphogenesis. Development *137*, 2177–2186.

Saurin, A.J., Shiels, C., Williamson, J., Satijn, D.P., Otte, A.P., Sheer, D., and Freemont, P.S. (1998). The human polycomb group complex associates with pericentromeric heterochromatin to form a novel nuclear domain. J. Cell Biol. *142*, 887–898.

Schuettengruber, B., Chourrout, D., Vervoort, M., Leblanc, B., and Cavalli, G. (2007). Genome regulation by polycomb and trithorax proteins. Cell *128*, 735–745.

Schuettengruber, B., Ganapathi, M., Leblanc, B., Portoso, M., Jaschek, R., Tolhuis, B., van Lohuizen, M., Tanay, A., and Cavalli, G. (2009). Functional anatomy of polycomb and trithorax chromatin landscapes in Drosophila embryos. PLoS Biol. *7*, e13.

Shen, C.N., Slack, J.M., and Tosh, D. (2000). Molecular basis of transdifferentiation of pancreas to liver. Nat. Cell Biol. *2*, 879–887.

Simon, J., Chiang, A., and Bender, W. (1992). Ten different Polycomb group genes are required for spatial control of the abdA and AbdB homeotic products. Development *114*, 493–505.

Simon, J., Chiang, A., Bender, W., Shimell, M.J., and O'Connor, M. (1993). Elements of the *Drosophila* bithorax complex that mediate repression by *Polycomb* group products. Dev. Biol. *158*, 131–144.

Soshnikova, N., and Duboule, D. (2009). Epigenetic temporal control of mouse *Hox* genes in vivo. Science *324*, 1320–1323.

Sprecher, S.G., and Desplan, C. (2008). Switch of *rhodopsin* expression in terminally differentiated *Drosophila* sensory neurons. Nature *454*, 533–537.

Struhl, G., and White, R.A. (1985). Regulation of the *Ultrabithorax* gene of Drosophila by other bithorax complex genes. Cell *43*, 507–519.

Tursun, B. (2012). Cellular reprogramming processes in Drosophila and C. elegans. Curr. Opin. Genet. Dev. *22*, 475–484.

Young, P.E., Richman, A.M., Ketchum, A.S., and Kiehart, D.P. (1993). Morphogenesis in Drosophila requires nonmuscle myosin heavy chain function. Genes Dev. *7*, 29–41.